

## Specific magnetic structure forming in polymer nanocomposites containing magnetite nanoparticles

T. S. Gendler<sup>1</sup>, A. A. Novakova<sup>2</sup>, and E. V. Smirnov<sup>3</sup>

Received 15 December 2004; revised 10 February 2005; accepted 1 March 2005; published 14 August 2005.

[1] The specific distribution of Fe<sub>3</sub>O<sub>4</sub> nanoparticles synthesized *in situ* in a polymeric PVA matrix was studied using the methods of magnetic measurements, transmission and depth-selective Mössbauer spectroscopy, and tunnel microscopy. The magnetic nanoparticles volumetric concentration  $C_v$  varied in the study samples from 0.6 vol. % to 43 vol. %. The size of the nanoparticles, measured using the X-ray diffraction, was found to be 10–20 nm. In the case of low  $C_v$  values the nanoparticles showed the composition of maghemite. At growing  $C_v$  concentrations, the product of the synthesis was partially oxidized magnetite. The contribution of the particles participating in the magnetic interaction at room temperature was estimated from the hyperfine magnetic splitting of the Mössbauer spectra. The blocking temperatures of the films of all compositions were found to be in the region of 300°C. This study revealed the high planar and linear magnetic anisotropy of the remanent saturation magnetization and of the remanent laboratory synthesis magnetization (LSM). The Mössbauer and microscopic studies revealed that during the synthesis the particles are distributed in the nanocomposite irregularly over the matrix, remaining almost isolated at the surface of the films and producing, in the lower part of the film, the chains of interacting nanoparticles, extending parallel to the film plain along the resulting trend. This chain structure is treated here as an artificial analog of fossil bacterial structures and biofilms, contributing to the magnetization of sedimentary rocks. **INDEX TERMS:** 1500 Geomagnetism and Paleomagnetism; 1594 Geomagnetism and Paleomagnetism: Instruments and techniques; 1518 Geomagnetism and Paleomagnetism: Magnetic fabrics and anisotropy; **KEYWORDS:** magnetic nanoparticles, thin films, magnetic properties, magnetic anisotropy.

**Citation:** Gendler, T. S., A. A. Novakova, and E. V. Smirnov (2005), Specific magnetic structure forming in polymer nanocomposites containing magnetite nanoparticles, *Russ. J. Earth. Sci.*, 7, ES4003, doi:10.2205/2005ES000177.

### Introduction

[2] The recent years witnessed that the researchers, dealing with the magnetism of the environment, with the paleomagnetism of sedimentary rocks and biomagnetism, grew interested in the magnetic behavior of nanostructures, that is, in the structures of natural and artificial origin, consisting of the ensembles of ultrafine ferrimagnetic particles with sizes corresponding to the nanoscale. In spite of their insignificant amount in the total mass of the material, the magnetic

nanoparticles of iron oxides and hydroxides play a significant role, for example, in surface sediments, in the enhancement of the magnetic signal in soil, providing information for climatic variations [Evans and Heller, 2003; Fassbinder *et al.*, 1990]. Ultradispersed iron oxides and sulfides provide a basis for the vital activity of magnetotactic bacteria and are the products of the activity of iron-reducing and iron-oxidizing bacteria. Changes in the contents of ultradispersed biogenic magnetite, both of intracellular and extracellular origin, in the sediments are the excellent indicators of changes in the oxidation-reduction conditions. This was traced, for example, in the bottom sediments of the Baikal Lake [Peck and King, 1996], in the western equatorial Pacific Ocean (ODP, Site 805) [Tarduno *et al.*, 1998], and in Lake Geneva [Gibbs-Eggar *et al.*, 1999] using the disappearance of bacterial magnetite at the iron-redox boundary. Along with the chemical processes operating in the near-surface environment, biogeocenosis results in the formation of films, both of organic and inorganic origin, inside and at the surface of sediments, soils, and rocks [Hancock, 2001]. The formation

<sup>1</sup>Institute of Physics of the Earth, Russian Academy of Science, Moscow, Russia

<sup>2</sup>Lomonosov State University, Department of Physics, Moscow, Russia

<sup>3</sup>Semenov Institute of Chemical Physics, Russian Academy of Science, Moscow, Russia

of biofilms contributes both to the generation of new minerals and to the destruction of the minerals contained in the rocks [De Long *et al.*, 1993; Krumbein *et al.*, 2003]. Changes can be introduced into paleomagnetic records also as a result of the formation of nanoparticle ensembles. It is not accidental that the problems of the role of nanoparticles in the environmental magnetism and the necessity of combining the methods of physics, chemistry, biology, and materials technology in the study of nanoparticle ensembles were included into the program of the Conventional Conference on Rock Magnetism held in Santa Fe in 2004 [see the paper by Jackson and Banerjee, 2004].

[3] The properties of the materials composed of nanoparticles, in particular their magnetic properties, differ fundamentally from those of their macroscopic analogs [Sohn *et al.*, 1998]. For instance, ultrafine particles show significantly lower values of specific saturation magnetization  $J_s$ , compared to their bulk analogs. In the case of magnetite nanoparticles this value is not higher than 30–60 Am<sup>2</sup> kg<sup>-1</sup>, compared to the bulk value of 92 Am<sup>2</sup> kg<sup>-1</sup> at room temperature [Sato *et al.*, 1987]. The  $J_s/J_{sbulk}$  value declines nonlinearly with a drastic decrease in the particle size region from 15–5 nm. This decline of saturation magnetization is associated by many researchers with the formation of so-called dead layers at the surface of the particles. For example, in the case of acicular maghemite particles the nonmagnetic boundary is inferred to be about 6 nm [Berkowitz *et al.*, 1968]; in the case of MnFe<sub>2</sub>O<sub>4</sub> particles 5.6 nm in size it was found to be 0.6 nm [Zheng *et al.*, 1998]. Moreover, the particles as small as that show hysteresis properties at room temperature and the paradoxical growth of the Curie temperature by 160 K compared to the bulk sample. This growth of the magnetic ordering temperature is believed to have been associated with the redistribution of the Mn and Fe cations in the tetra- and octahedral sublattices of the spinel structure in the thin boundary layer. The example of another specific feature of the magnetic properties of thin magnetite films, 50 nm thick, at the MgO surface, is the absence of saturation in the fields as high as 7T, which is believed to have been associated with the high density of the resulting antiphase domain boundaries [Rudee *et al.*, 1997]. The exchange interaction at the boundaries of this type changes compared to the bulk Fe<sub>3</sub>O<sub>4</sub> with the origin of a new 180° Fe-O-Fe interaction which leads to antiferromagnetic coupling at the boundaries of the domains [Voogt *et al.*, 1998]. The growing interest in studying the peculiar properties of magnetic nanoparticles is proved by the great number of papers presented at several sections of the International Conferences on Magnetism (ICM-2003, ICM-2004). The analysis of these papers shows that in terms of the nanosizes the differences between amorphous, disordered, solid and even between biological structures become insignificant. Very productive in this connection is the use of modern supersensitive methods of physics, chemistry, biology, and materials technology for studying the products of biogeochemical processes and their artificial analogs. A significant role in this case belongs to laboratory modeling in the field of inorganic surface chemistry and, in particular, to the synthesis of polymeric nanocomposites. As proved by some researchers [Sohn *et al.*, 1998], these materials show new magnetic properties,

produced both by the size effects and by the significant role of the polymeric matrix. The study of the regular distribution and behavior of ferrimagnetic particles in the matrix of this kind, which is taken here as an analog of the intracellular or extracellular organic matter of the envelopes of biomineralized particles in nature, may throw light on the mechanism of the formation and magnetic properties of bacterial magnetosomes and biofilms.

[4] Reported in this paper are some of the results obtained during the study of the magnetic properties of nanocomposite materials based on polyvinyl alcohol (PVA) and magnetite nanoparticles [Gendler *et al.*, 2004; Novakova *et al.*, 2002, 2003, 2005a, 2005b].

## Preparation of Samples and the Methods of Their Study

[5] The polymer nanocomposites examined in this study had been synthesized at the Chemical Faculty of the Moscow State University in Petri dishes in the ambient laboratory magnetic field, disregarding its direction. The synthesis was made using a 4% PVA water solution with the addition of a mixture of FeCl<sub>2</sub>·4H<sub>2</sub>O and FeCl<sub>3</sub>·6H<sub>2</sub>O (with a molar ratio Fe<sup>2+</sup>/Fe<sup>3+</sup>=0.5) dissolved in water. As a result of this reaction and after the addition of a six-percent NaOH solution and a gel-forming agent, Fe<sub>3</sub>O<sub>4</sub> nanoparticles were formed. The resulting gel varied in color during 5–10 minutes from reddish brown to black, depending on the concentration of iron oxide in the samples. This proved the *in situ* formation of not only magnetite particles but also of maghemite and partially oxidized magnetite particles. After the 24-hour storage of the gel in a closed Petri dish, the gel was washed with water for a long time and then dried in air at room temperature for 3–5 days. This resulted in the formation of polymer films, 200 μm thick, with iron oxide nanoparticles distributed over their volumes. In the course of the drying of the films the latter changed in color, this potentially being caused by the air access. To sum up, the real composition of the nanoparticles in the synthesized polymer films could be determined only in further studies. Conventionally, the particles were identified as magnetite, and their calculated volumetric ( $C_v$ ) and weight ( $C_p$ ) concentrations were referred to Fe<sub>3</sub>O<sub>4</sub>. Several syntheses of this kind were performed. As a result we got nanocomposite samples with different volumetric concentrations of Fe<sub>3</sub>O<sub>4</sub> nanoparticles (from  $C_v = 0.6\%$  to  $C_v = 43\%$ ), this corresponding to the  $C_p$  values varying from 2.4% to 75.4%. The total number of samples examined in this work was ten samples with different concentrations obtained from three syntheses. The composition and size of the crystalline grains, the homogeneity of the distribution of particles in the film sequences, and the magnetic state of the nanoparticles were determined using X-ray diffraction, a number of methods used to study rock magnetism, and transmission and depth-selective Mössbauer spectroscopy.

[6] The macroscopic magnetic characteristics of the films, such as saturation magnetization ( $J_s$ ), remanent saturation magnetization ( $J_{rs}$ ), natural remanent magnetization

( $J_n$ ), as well as their temperature dependence  $J_s(T)$  and  $J_{rs}(T)$ , were carried out in the Geomagnetic Laboratory of the Institute of Physics of the Earth, Russian Academy of Science, using a JR-4 magnetometer (AGIKO), a vibromagnetometer (VSM), and a two-component laboratory thermomagnetometer (Orion Company, Borok). The magnetic field used to produce  $J_s$  and  $J_{rs}$  was equal to 450 mT. The coercive force ( $H_c$ ) and the remanent coercive force ( $H_{cr}$ ) were measured using a coercimeter in the maximum magnetic field of 1.7T (Orion Company, Borok). In this case  $J_n$  denotes the magnetization acquired by the films during the laboratory synthesis in the ambient geomagnetic field. Conventionally, we will refer to this magnetization as laboratory synthesis magnetization (LSM). In order to obtain the LSM vector and  $J_{rs}$  characteristics and study the anisotropy of these types of magnetization we measured the films in a cubic nonmagnetic organic glass container in three orthogonal directions X, Y, and Z. The Z axis was taken to be perpendicular to the film, the X and Y axes residing in the film plane. Since this synthesis was carried out without fixing the direction of the Earth magnetic field, the direction of the maximum values of the LSM and  $J_{rs}$  vectors in the film plane was chosen after the measurements to be the X-axis.

[7] The Mössbauer transmission spectra were obtained in the laboratory of the Solid State Physics Department, Moscow State University, using a spectrometer of constant acceleration. The radioactive source was  $\text{Co}^{57}(\text{Rh})$ , the velocity scale of the spectrometer was calibrated using a standard  $\alpha\text{-Fe}$  absorber. All experimental spectra were subject to compute fitting using a special program based on the Lorentz form of spectra lines. To check the homogeneity of the particle distributions of over the thickness of the film, Mössbauer spectra were obtained for different thicknesses below the surfaces of the study samples. Depth selective Mössbauer spectroscopy was performed in the geometry of back scattering with registration of two types of secondary radiation: conversion electrons (information from the subsurface layer  $\sim 0.3 \mu\text{m}$ ) and conversion X-ray (information from the subsurface lay  $\sim 20 \mu\text{m}$ ) [Kuprin and Novakova, 1992].

## Discussion of the Results

[8] The diffractograms obtained for the samples of all compositions showed a system of lines of a cubic spinel structure with broad reflections, typical of magnetite or maghemite. The analysis of the resulting X-ray diffraction line widenings, performed using the Scherrer formula [Araki, 1989] showed the average size of the particles in the regions of their low concentrations to be 10 nm. In the regions of their higher concentrations the average size of the particles was as high as 25 nm, obviously because of their growing coagulation. This was accompanied by the order-of-magnitude growth of microtension [Novakova *et al.*, 2002, 2003]. The significant broadening of the lines complicated the reliable distinction between magnetite and maghemite with disordered vacancies. No superstructural reflections, typical of ordered

maghemite, were found, this being another typical feature of ultradispersed particles [Haneda and Morrish, 1977].

[9] The Mössbauer transmission spectra, obtained at room temperature ( $T_r$ ), showed substantial gradual changes with the growth of magnetite nanoparticles concentration (Figure 1). In the case of low  $C_v$  values the significant part of the spectra were occupied by doublets corresponding to noninteracting superparamagnetic particles of magnetite against the background of unresolved, low-intensity hyperfine magnetic splitting. With the  $C_v$  growth the intensity of the magnetically split portion of the spectrum ( $S_{\text{magn}}$ ) grows higher, indicating the growing contribution of the particles involved in magnetic interaction. The  $S_{\text{magn}}$  growth calculated after the computer processing of the results was found to be monotonic (Figure 2a).

[10] In contrast to the X-ray diffraction, the Mössbauer spectroscopy showed the high oxidation of the magnetite particles in polymer film, especially in the case of low  $C_v$  concentrations. The magnetically split spectra obtained for low  $C_v$  concentrations (3–11%) are symmetrical and agree in terms of their parameters only with the content of  $\text{Fe}^{3+}$  ions in the study maghemite. In the case of higher  $C_v$  concentrations the increased resolving of the first two lines of the spectrum was observed, which is characteristic of magnetite. The isomeric shifts, obtained for various sextets after the computer fitting of the spectra also identify the material to be magnetite. However, even at the highest  $C_v$  values, such as 33% and 43%, the ratio between the spectral intensities for tetra- and octahedral sublattices ( $S_A/S_B$ ) are larger than 1, which does not correspond to stoichiometric magnetite ( $S_A/S_B = 0.5$ ). Therefore the particles produced by synthesis and subsequent drying are composed of maghemite in the case of low  $C_v$  values and of oxidized magnetite in the case of high  $C_v$  values.

[11] Proceeding from the visual observations of changes in the color of the films in the course of their preparation and from the results of the Mössbauer spectroscopy, it can be inferred that in the case of the low concentration of iron salts in the solution, the partial oxidation of magnetite nanoparticles occurred as early as at their transformation to gel and ended during drying, because scattered in the isolation manner in the cooling polymer material, the nanoparticles have high specific surface. With the growth of the salt concentration in the solution up to 20% and higher, the formation rate of ferrimagnetic particles increases resulting in their ability to produce agglomerates with a lower specific surface. As a result, during the gel formation, the particles remained to be composed of magnetite, yet, the drying of the composite material showed partial single-phase oxidation or the formation of maghemite films at the surface of the magnetite nanoparticles. In the latter case, the particles showed a two-phase, coherently conjugated magnetite-maghemite system. The similar synthesis of magnetite nanoparticles, about  $\sim 10\text{--}15 \text{ nm}$  in size, without the participation of any polymer, resulted in the complete oxidation of the primary magnetite with the spectra showing no indications of magnetite components [Novakova *et al.*, 1992]. The spectra of nonstoichiometric magnetite, similar to those obtained for the samples with  $C_v = 33\text{--}43\%$ , were observed by Jolivet *et al.* [1992] during the synthesis of magnetite from a  $\text{FeCl}_2$  and  $\text{FeCl}_3$  salt

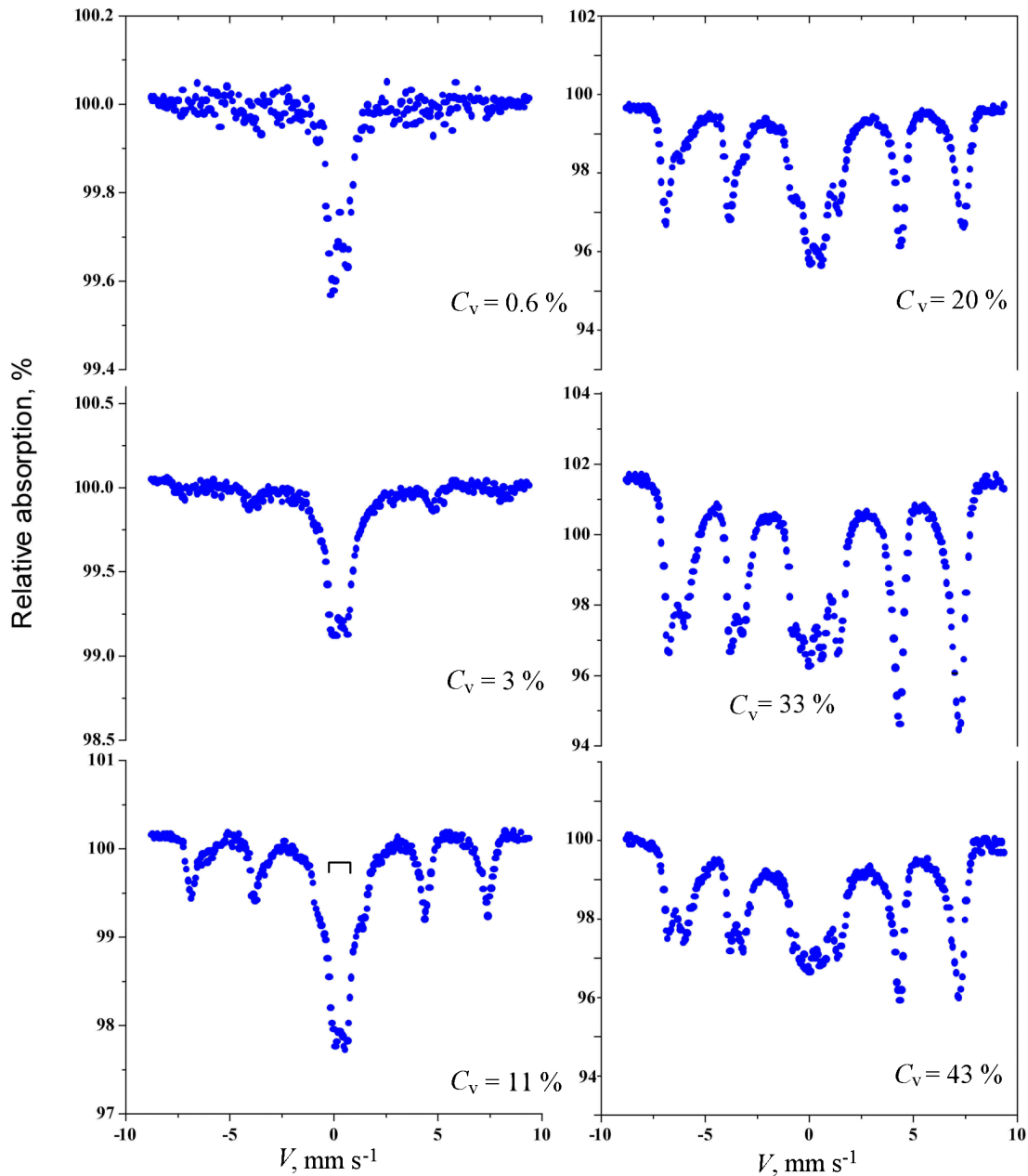


**Figure 1.** Mössbauer transmission spectra of polymer films with different volumetric concentrations of magnetite ( $C_v$ ) at room temperature.

solution with  $\text{Fe}^{2+}/\text{Fe}^{3+} = 0.30\text{--}0.50$  without polymer participation, yet in the  $A_r$  atmosphere, which precluded potential oxidation. The size of the synthesized particles varied from 4 nm to 20 nm, or from  $\sim 8.5$  nm to 20 nm as indicated by electron microscopy. The PVA solution was added to the resulting suspension to produce films for Mössbauer spectroscopy.

[12] The similarity of the spectra obtained in our study and those reported by *Jolivet et al.* [1992] suggests that in the case of high iron salt concentrations in the solution the PVA addition in the course of the reaction precludes the

complete oxidation of nanoparticles. However, this is not the only effect of the polymer. Numerous Mössbauer studies of fine-dispersed maghemite particles varying little in size (6–10 nm), demonstrated that the spectra obtained at room temperature showed either a paramagnetic doublet or partial relaxation effects characteristic of systems with noninteracting supermagnetic particles [*Coey and Khalafalla, 1972; Mørup, 1990; Pankhurst, 1994*]. In the cases where the particles synthesized from salt solution were coated with oleic acid, 1.0–1.5 nm thick, the relative doublet content grew substantially compared to the pressed uncoated particles

[Mørup, 1990]. This proved the lower magnetic interaction among the coated particles. Our study showed a different situation: with a significant separation of particles by a polymer at the synthesis stage (the  $C_v$  values being lower than or equal to 11%) the spectra demonstrated stable magnetic interaction between some of the iron oxide particles. The number of these particles increased with the growth of their total volumetric concentration ( $C_v$ ). The same type of magnetic splitting, “prohibited” for the isolated particles of this size, was observed in the case of monocrystalline magnetite layers merely 5.3 nm thick at the MgO surface [Voogt, 1998].

[13] The specific feature of the spectra of the polymer films examined, in spite of their external similarity with the spectra obtained for a bulk magnetite, was the low values of the hyperfine magnetic fields ( $H_{hf}$ ). This lowering was especially significant where the contribution of the superparamagnetic doublet was low and the relaxation was absent, and, hence, cannot be explained in terms of superparamagnetic relaxation. The  $H_{hf}/H_{hf(bulk)}$  ratios for the  $Fe^{3+}$  in the films with the low  $C_v$  concentrations (3–5.7%), where the particles showed the best isolation, was found to be 0.96–0.94; it declined from 0.9 to 0.86 as the  $C_v$  value grew from 11% to 43%. A similar trend of the  $H_{hf}$  decline, with the paramagnetic doublet declining to zero, was reported by Jolivet *et al.* [1992] and Voogt *et al.* [1998]. The  $H_{hf}$  decline is a specific feature of the physics of nanoparticles and thin layers. The magnetic interaction in the case of particles is more controlled by the extent of their isolation than grain size [Mørup, 1990]. In the present case the effects responsible for the lowering of hyperfine magnetic fields is the active role of a polymer matrix which, on the one hand, separates the conglomerates of interacting nanoparticles and, on the other hand, have an influence on the exchange interaction because of medium elastic forces.

[14] The specific saturation magnetization of films ( $J_{sf}$ ), measured in the magnetic field of 450 mT (the lower curve in Figure 2b), demonstrates also its monotonous growth with the growing  $C_v$  value in a broad range of the values varying from 0.47  $Am^2 kg^{-1}$  to 60  $Am^2 kg^{-1}$ . The scatter of the  $J_s$  values for different pieces of the film of the same composition amounts to 20–25%, this possibly being caused by the nonuniform distribution of the nanoclusters inside the polymer material. Since the measured magnetization values are controlled primarily by the concentration of ferrimagnetic particles, the monotonic  $J_{sf}$  growth proves the validity of the volumetric  $C_v$  concentrations in the case of different batches. Despite the insignificant polymer weight, the  $J_{sf}$  value of the films is much lower than that of magnetite (92  $Am^2 kg^{-1}$ ) and than that of maghemite (74  $Am^2 kg^{-1}$ ).

[15] In computing the true specific value of the saturation magnetization of any ferromagnetic phase, formed in the course of the reaction, the unknown value is the mass of nanoparticles contributing to the measured  $J_s$  value. In the case discussed, to calculate the  $J_s$  values of nanoparticles ( $J_{sn}$ ), the magnetization values measured for the specimens, for which Mössbauer spectra had been obtained, were corrected in two stages. The first correction stage was based on the formal view that the only mineral produced as the result of the reaction had been magnetite the weight percentage of which ( $C_p$ ) was calculated for each individual synthesis, pro-

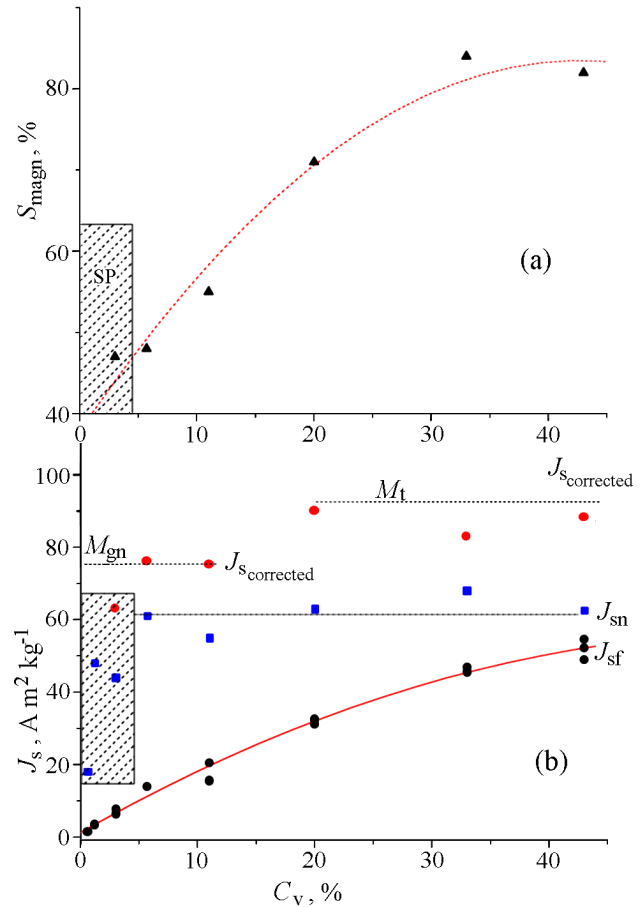


**Figure 2.** (a) shows the relative area of magnetically split  $S_{magn}$  components (%) in the Mössbauer spectra of the films with different iron oxide concentrations ( $C_v$ ). The shaded rectangles denote the rock compositions whose spectra are represented by a superparamagnetic (SP) doublet; (b) the saturation magnetization values ( $J_s$ ) for the films with different volumetric  $C_v$  concentrations: the black circles denote the values of specific saturation magnetization of the films ( $J_{sf}$ ); the blue squares, the specific saturation magnetization of nanoparticles calculated using the weight content of magnetite  $C_p$ , the latter was estimated proceeding from the contents of the components developed in the course of the film synthesis; the red solid circles denote the specific saturation magnetization of real maghemite particles (for  $C_v$  values lower than or equal to 11%) and those of magnetite (for  $C_v$  values lower than or equal to 20%). These calculations were made only using corrections for the magnetically ordered particles in the samples (Figure 2a). The broken lines are drawn to mark the values characteristic of maghemite and magnetite bulk compositions. The shaded rectangle is shown for the values, most of the spectra of which were represented by SP doublets. Therefore, the correction procedure involving  $S_{magn}$  could not be performed or was associated with significant errors.

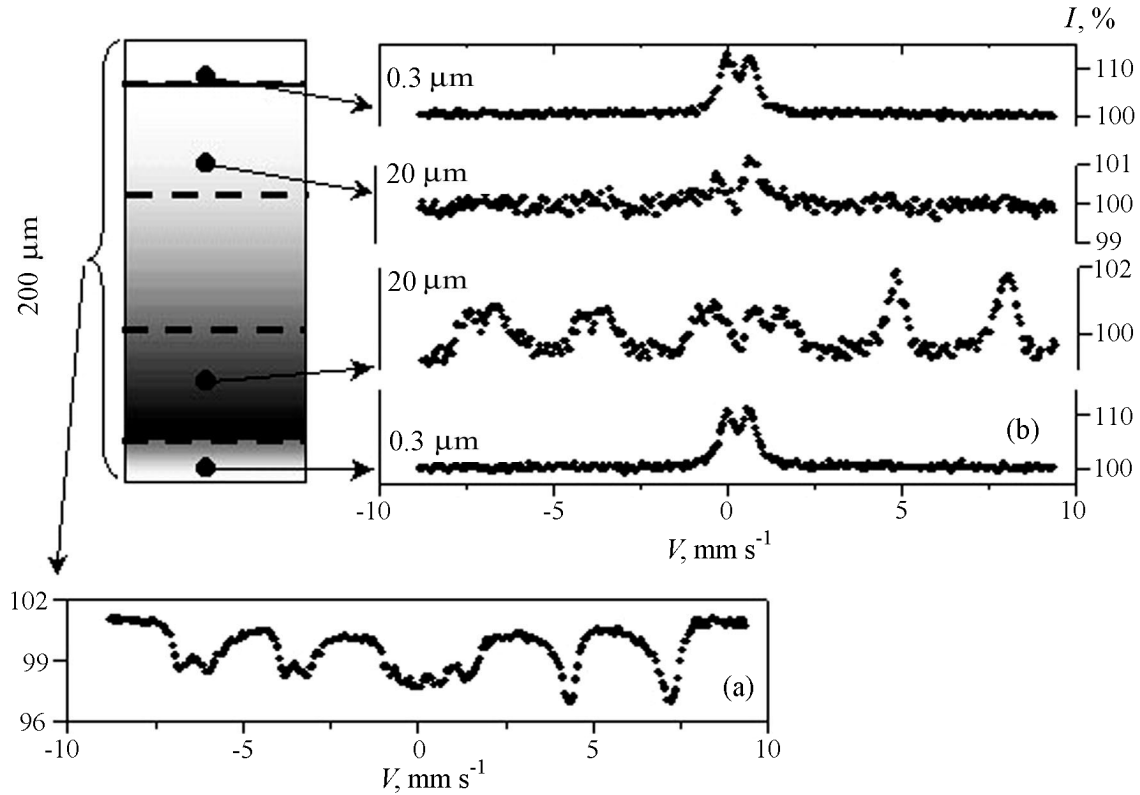


**Figure 3.** Mössbauer depth selective analysis of the sample with  $C_v = 33\%$ : (a) transmission spectrum for the whole thickness of sample, (b) conversion electron and X-ray spectra for the subsurface layers, 0.3  $\mu\text{m}$  and 20  $\mu\text{m}$ , of the both film sides.

ceeding from the amounts of the respective components in the solution. The results of the  $J_{sn}$  computation are shown in blue color in Figure 2b. One can see that the  $J_{sn}$  values are higher than the respective  $J_{sf}$  values and show two intervals of the peak  $J_{sn}$  values: 18–48  $\text{Am}^2 \text{kg}^{-1}$  for the  $C_v$  values lower or equal to 3% and 55–65  $\text{Am}^2 \text{kg}^{-1}$  for the  $C_v$  concentrations higher or equal to 5.7%. These values are lower than the  $J_s$  values of magnetite or maghemite. In this connection, the samples with purely paramagnetic spectra ( $C_v = 0.6\%$  to 1.2%) were discarded because the contribution of SP particles, stabilizing in the magnetic field during  $J_s$  measurements, could not be estimated correctly.

[16] In the case of the other film compositions the mass was calculated including the percentage of the particles that participated in magnetic interaction, this being determined from a ratio between the areas of the magnetic and superparamagnetic components in the spectra (Figure 2a). In this case the weight percentages ( $C_p$ ) of the ferrimagnetic phases of the samples with the  $C_v$  values of 3% and 5.7% were recalculated for maghemite in accordance with the spectroscopic data available. The values obtained after the second stage of corrections ( $J_s$ ) also showed two groups (red dots in Figure 2b). One group, corresponding to the low concentrations, was located in the vicinity of the  $J_s$  value obtained for maghemite.

[17] The other group of the corrected  $J_s$  values resided

in the region of 82–89  $\text{Am}^2 \text{kg}^{-1}$  which accounted for 0.90–0.96 of the  $J_s$  value obtained for stoichiometric magnetite and can be easily explained for the case of nonstoichiometric magnetite or for the case of a two-phase  $\gamma\text{Fe}_2\text{O}_3 + \text{Fe}_3\text{O}_4$  system. A more exact calculation was found to be possible only after getting a few versions of the computer processing of the spectra, which was beyond the scope of this paper. Our correction procedure proved that the use of the results of merely macroscopic magnetic measurements may lead to the underestimation of the specific magnetic saturation of ferrimagnetic nanoparticles.

[18] As mentioned in the introduction to this paper, the underestimated values of specific saturation magnetization is a characteristic feature of the physics of nanoparticles of ferrimagnetic materials and thin films, which is a subject of discussion in the modern literature. Various models, often precluding one another, are offered to explain this effect. The examples are the formation of magnetically inactive or magnetically dead layers at the surface of the particles; changes in the cation distribution; the noncolinearity of spins in the A and B sublattices; variations of the  $K_1$  crystallographic anisotropy constant; the fragmentary distribution of cation sublattices with the preservation of a continuous  $\text{O}^{2-}$  sublattice; and the antiphase boundaries precluding ferrimagnetic interactions among magnetic domains and producing their patchworks [Coey and Khalafalla, 1972; Goss, 1998; Han

*et al.*, 1994; Mørup, 1990; Pankhurst, 1994; Voogt, 1998; Zheng *et al.*, 1998]. In the case of polymer nanocomposites two coexisting versions can be proposed, instead of complex models, to explain the underestimation of  $J_s$  nanoparticles. One of them is the heterogeneous distribution of particles in terms of their sizes in the course of the synthesis, where only a small number of the particles have a superparamagnetic size. The other version is the heterogeneous distribution of nanoparticle clusters, both over the film thickness and inside the layers (isolated noninteracting particles and the conglomerates of interacting ones). The former proposition is based on the general considerations and on the results of the suspension fractionation study performed by Jolivet *et al.* [1992] after the similar synthesis of magnetite without any polymer participation. The latter was confirmed by the study of film layers using depth-selective Mössbauer spectroscopy [Novakova *et al.*, 2003, 2005b].

[19] The conversion Mössbauer spectra were collected from both sides of the studied polymer films at the surface and at a depth of a 20-micron thick layer. Figure 3 shows the results of the study of this kind for a sample with the  $C_v$  concentration of 33%. One can see from this figure that the spectra obtained for different thicknesses of the film differ substantially. It is worth mentioning that the thin surface layers on both sides of the film showed similar doublet spectra indicating the absence of magnetic interaction among the superparamagnetic iron oxide particles. It appears that the particles in the surface layers are scattered for higher distances from one another. The layers 20  $\mu\text{m}$  thick showed different spectra. The upper layer showed mainly a doublet component at the background of poor hyperfine magnetic splitting. However, the spectrum of the lower layer of the same thickness showed a clearly expressed magnetic structure typical of the magnetite spectrum. Its form coincides almost wholly with the spectrum obtained for the total thickness of this sample, shown in the same figure. These experiments demonstrate clearly the heterogeneous distribution of particles in the course of the synthesis in a polymeric material and, as a consequence, a difference in their magnetic interactions.

[20] Although most of the particles are located in the lower 20-micron film layer, this layering cannot be identified as exceptionally gravitational one, because the spectra of the subsurface layers are identical. It can be supposed that the surface layers of the film grow faster than the internal ones. The slower drying of the internal part of the film seems to produce conditions favorable for the agglomeration of the particles separated by the polymeric material. In this case, in spite of the superparamagnetic size of the particles, magnetic interaction exists inside the agglomerate. Similar aggregates of magnetite particles, of a few nanometers, were observed in the case of the bacterial reduction of amorphous ferric hydroxide [Fredrickson *et al.*, 1998]. The theory of exchange interaction between the closely spaced particles of superparamagnetic size was offered by Mørup [1990], and this interaction phenomenon itself was referred to superferromagnetism. It is obvious that in the case of nanocomposite materials the decisive role in the magnetic interaction of nanoparticles is played by a polymer and its elastic characteristics. As follows from Figure 3, the organizing effect of

**Table 1.** The results of processing the  $J_s(T)$  curves

$C_v$	$\alpha$	$T_1$	$T_2$	$T_2 - T_1$	$T_{cf}$	$T_c$
3	0.42	211	298	87	457 (lin)	532 (4)
11	0.30	218	327	109	425 (4)	523 (8)
20	0.23	217	334	117	352 (4)	526 (8)
33	0.19	231	363	132	415 (4)	518 (8)
43	0.18	215	366	151	450 (4)	518 (8)

Note:  $\alpha = J_{sf_0} - J_{sf}(200) / J_{sf_0}$  is the parameter characterizing the steepness of the  $J_{sf}(T)$  curves for the first heating;  $T_1$  and  $T_2$  are the temperatures of the beginning and end of the film destruction;  $T_{cf}$  is the virtual Curie temperature in the film determined by the extrapolation of the initial segment of curves  $J_{sf}(T)$ ;  $T_c$  is the Curie temperature of the nanoparticles after the destruction of the film, found from the first derivative; given in the parenthesis is the degree of the polynomial describing this segment of the  $J_{sf}(T)$  curves; lin – linear.

the polymer in this kind of synthesis develops slowly in a  $20 < d \leq 180$  micrometer layer, where both surfaces can be classified as “dead layers”.

[21] The shapes of the saturation magnetization vs. temperature curves and the measured  $T_c$  values provide additional information for the type of the magnetic interaction among fine-dispersed particles. In the case of polymer films containing magnetite or maghemite particles some difficulties arise in association with the fact that the temperature of the polymer destruction may be lower than that of the destruction of the magnetic order in the ensemble of the particles. Nevertheless, in the study reported here the thermomagnetic  $J_s(T)$  curves were measured in the temperature interval of 20–700°C in the cases of all film compositions. The examples of the normalized curves obtained during the first and second heatings are shown in Figure 4, the results of their processing being summarized in Table 1. The first feature that attracts attention in the behavior of the first-heating curves is a break in their monotonic behavior in the  $T_1 - T_2$  temperature interval, associated with the destruction of the polymer. The  $T_1$  temperature varied from 211°C to 231°C and  $T_2$ , from 298°C to 366°C, for the films of different compositions. The  $T_2 - T_1$  interval grew regularly with the growth of the volumetric iron oxide concentration. Another peculiar feature of the curves behavior was the difference in their steepness prior to and after the break, this proving the different type of the magnetic interaction between the particles in the film prior to and after its decomposition. Since it was impossible to connect the segments of the curves obtained for the situations prior to and after the break, the curves were processed using polynomials in the segments of (20°C) –  $T_1$  and  $T_2 - (600^\circ\text{C})$ . It was found that in the case of the compositions with the  $C_v$  values varying from 0.6% to 3% their curves were approximated in an excellent way by a linear function in the former segment, and in the case of the compositions with  $C_v \geq 11\%$ , by the polynomials of grade 4. The second segment of the curves could be approximated adequately by grade-4 polynomials in the cases of  $C_v$  values equal to or lower than 3% and by grade-8 polynomials in the case of the  $C_v$  equal to or higher than 11% (Table 1, figures in brackets). Variations in the shapes of the  $J_s(T)$  curves in

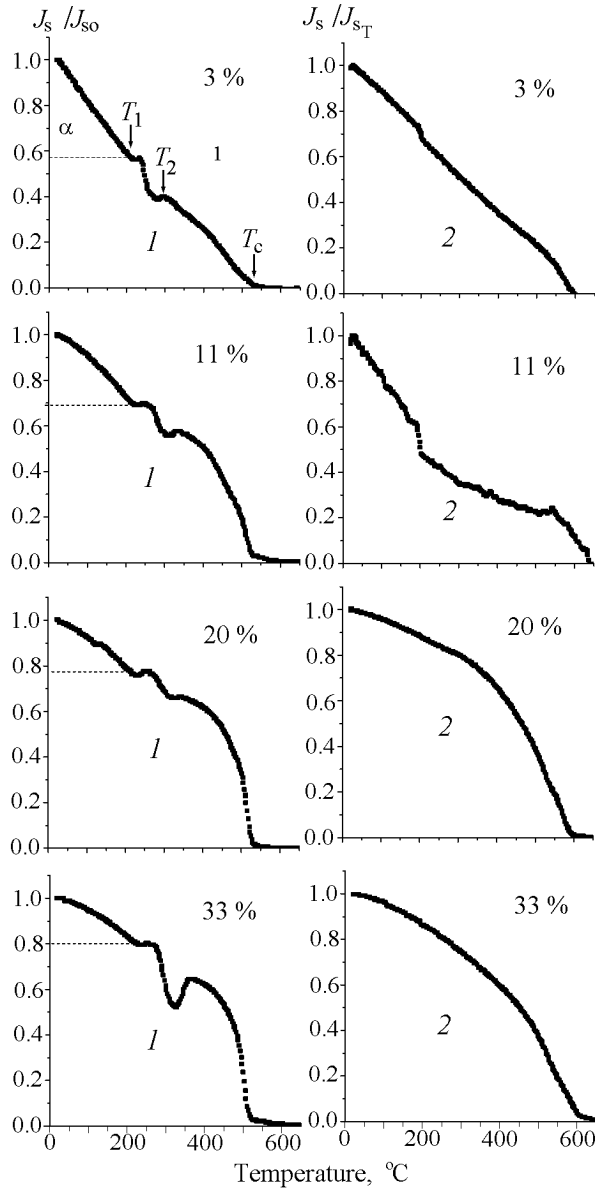


**Figure 4.** Normalized thermomagnetic  $J_{sT}/J_{s0}(T)$  curves for the films with different concentrations of  $C_v$  nanoparticles. The left column shows the data obtained for the first heating, the right one, for the second heating.  $T_1$  and  $T_2$  denote the temperatures of the beginning and end of the polymer destruction, used in the mathematic processing of the curves using polynomials.  $T_c$  is the Curie temperature. The alpha symbol denotes the amount of the saturation magnetization, demagnetized by heating to 200°C.

the first segment were caused by the substantial content of superparamagnetic particles in the case of the low content of iron oxide in the film. In the case of its higher concentrations magnetic interaction remained to be high enough in spite of the fine size of the particles. As an additional parameter

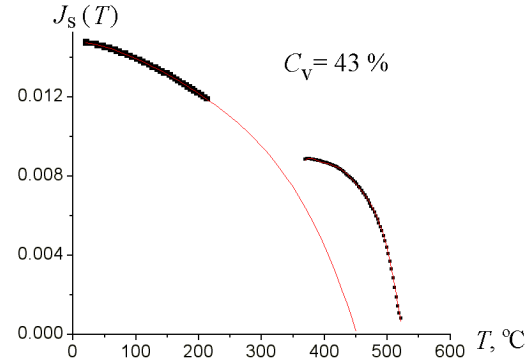


**Figure 5.** Example of the mathematical processing (using polynomials) of the segments of the experimental thermomagnetic  $J_s(T)$  curve for a film with  $C_v = 33\%$ . The upper segment of the curve was interpolated by a polynomial of grade 4, the lower, using a polynomial of grade 8. The break in the curve denotes its segment which was discarded because the polymer material was destroyed.

( $\alpha$ ), controlling magnetic interaction between the nanoparticles in the film, we preferred to use the decline of the initial saturation magnetization  $J_{sf0}$  as a result of heating to the temperature of 200°C:  $\alpha = J_{sf0} - J_{sf}(200)/J_{sf0}$ . As shown in Table 1, the  $\alpha$  value diminishes with the growing volumetric concentration of particles in the film, this indicating the growth of magnetic interaction. In the case of massive magnetite,  $\alpha = 0.09$  in this temperature interval.

[22] For the formal determination of the Curie temperatures of the films, the polynomials of the first segment were extrapolated for a greater temperature range, and the point of the intersection with the temperature axis was assumed to be  $T_{cf}$ . An example of this extrapolation is shown in Figure 5 for the composition with  $C_v = 43\%$ . The  $T_c$  values determined after this procedure were in the range of 415–457°C, without of any visible correlation with  $C_v$ . The exclusion was a sample with  $C_v = 20\%$ , for which the computed  $T_{cf}$  value was 352°C. The virtual point of the intersection of the two  $J_s(T)$  curve branches could also be taken to be the Curie temperature. In this calculation procedure the  $T_{cf}$  values were in the vicinity of 300°C. It could be supposed that the temperature of about 300°C was not the Curie temperature of the films, but the temperature of maghemite to hematite transition. However, the saturation magnetization did not decline after the cooling from 300°C, this allowing one to interpret the computed  $T_{cf}$  values as Curie temperatures. In this case the particular  $T_{cf}$  values are not important. What is important is the fact that in the cases of all nanoparticle concentrations in the films the Curie temperatures are higher than the room temperature, yet, lower than that of bulk magnetite ( $T_c = 585^\circ\text{C}$ ). It follows that in the case of a high outer magnetic field the superexchange magnetic interaction of nonstoichiometric magnetite particles, “frozen” in the films, is fairly strong, yet weaker than in massive magnetite or maghemite. This weakening of the exchange interaction explains the above-mentioned decline of the  $H_{hf}$  values in the Mössbauer spectra of the films.

[23] The Curie temperatures ( $T_c$ ) of the free-particle conglomerates that remained after the destruction of the polymer were determined using the first derivatives of the experimental curves. The  $T_c$  values were found to decline from 532°C to 517°C with the growth of the  $C_v$  concentration. These values were also lower than the  $T_c$  values of the bulk stoichiometric and, moreover, nonstoichiometric magnetite or maghemite. It could be supposed that the destruction of the film and the surface liberation of the particles was followed by the further oxidation or their sintering of the fine-dispersed particles. However, as follows from the  $T_c$  measurements, no substantial oxidation or welding of the particles were observed prior to the heating to 600°C. It was only after the heating up to 700°C and the cooling down to room temperature, that the  $J_{sfT}$  values declined by factors of 2 to 7 ( $J_{sfT}/J_{sf0} \sim 0.15 - 0.5$ ), the Curie temperatures of the resulting mineral phase being close to 600°C (see the right-hand column in Figure 4). In some cases the curves had tails up to 650°C. Although the  $J_{sf}$  value declined significantly, the specific values of this parameter, calculated for the weight content of magnetite or maghemite, were higher than 10 Am<sup>2</sup> kg<sup>-1</sup>. Hence, most of this magnetization belonged to the particles of oxidized magnetite or maghemite, that is, the analyzed material was not fully transformed to hematite during the heating of the films. The exception was a sample with  $C_v = 11\%$ , whose  $J_s$  value was found to be 50 times lower, and whose second-heating  $J_s(T)$  curve was obviously of a two-phase type and showed the high content of hematite (Figure 4).

[24] The significant role of polymer in the stable magnetic interaction of nanoparticles was manifested even more obviously during the study of the remanent magnetic characteristics of films [Novakova *et al.*, 2003, 2005a]. In the case of magnetite nanoparticles,  $\sim 10$  nm in size, derived from GS-15 bacteria, the blocking temperature ( $T_b$ ) was found to be lower than the room temperature [Moscowitz *et al.*, 1989]. The hyperfine magnetic splitting in the film spectra at room temperature ( $T_r$ ) cannot, in principle, be interpreted as contradictory, because the relaxation times  $\tau$  for magnetic and Mössbauer measurements are not much different (about 10<sup>2</sup> s and about 10<sup>-8</sup> s, respectively). This difference diminishes more than four times the  $T_b$  values observed in magnetic measurements, compared to Mössbauer ones. For instance, in the case of maghemite nanoclusters, 5 nm in size, in block copolymer, the  $T_b$  values derived from magnetic and Mössbauer measurements were found to be 16 K and 50 K, respectively. Hence, it was natural to infer the absence of hysteretic properties in the study films. However, all of the samples showed the measurable  $J_{rs}$ ,  $H_c$ ,  $H_{cr}$ , and LSM values even in the cases of the lowest iron oxide concentrations. This is another proof of the existence of magnetic interaction between the nanoparticles separated by a polymer, which results in the formation of a specific domain structure in the films.

[25] The blocking temperatures of the films ( $T_{bf}$ ) were derived from the  $J_{rs}(T)$  curves, the examples of which are shown in Figure 6. The concave shapes of the curves with  $T_b$  values of about 300°C characterize the fine dispersion of the particles even in the cases of their highest concentrations in the films. As mentioned above, we must certainly bear in

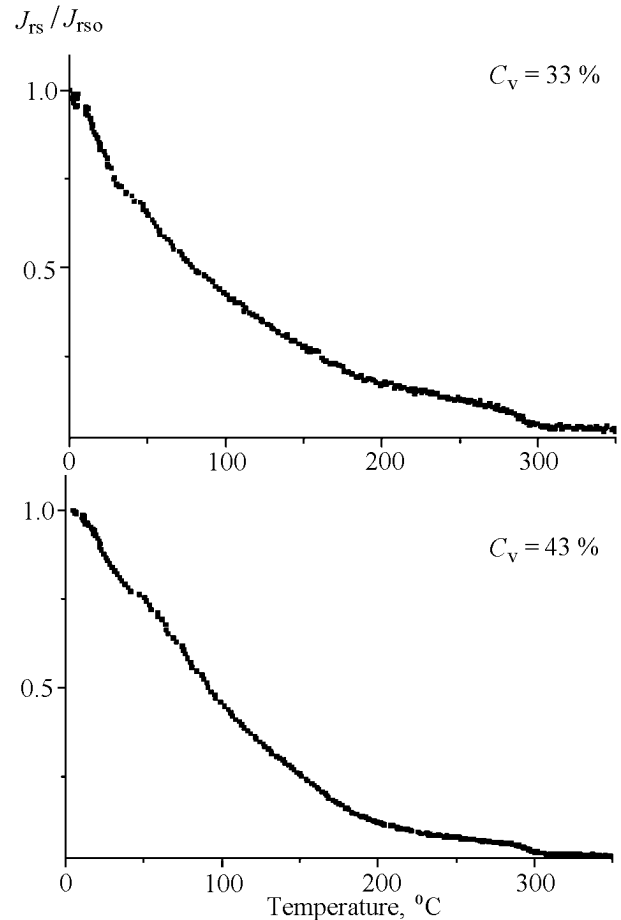


**Figure 6.** Normalized thermomagnetic curves of the remanent saturation magnetization  $J_{rs}/J_{rso}(T)$  of the films with the nanoparticle concentrations of 33% and 43%.

mind that  $T \sim 300^\circ\text{C}$  is simultaneously the temperature of the polymer destruction in the case of the heating as long as this one. However, the monotonous decline of the  $J_{rs}$  value to zero in the course of heating, as well as the stability of the  $J_{rs}$  values after the cooling from 400°C to the room temperature, allow one to rank  $T \sim 300^\circ\text{C}$  as a true blocking temperature.

[26] In contrast to the  $J_{sf}$  value, the specific  $J_{rsf}$  values of the films showed a nonmonotonic variation with the growth of the  $\text{Fe}_3\text{O}_4$  concentration. It attained its maximum value where  $C_v$  was equal to 20% and declined with its further growth (Figure 7a). The nonsporadic recording of the  $J_{rsf}$  behavior at  $C_v = 20\%$  and its decline at higher concentrations was confirmed by the measurements performed using samples with the  $C_v$  values equal to 18% and 31% obtained during the repeated synthesis. This phenomenon remains to be clarified. The  $J_{rs}$  values obtained for different concentrations were compared at the time interval of 80 s after the magnetization because significant magnetic viscosity was observed [Novakova *et al.*, 2003]. The nonmonotonous character of the  $J_{rsf}$  variation showed good correlation with the variations of  $H_c$  and  $H_{cr}$  values (Figures 7b and 7c),

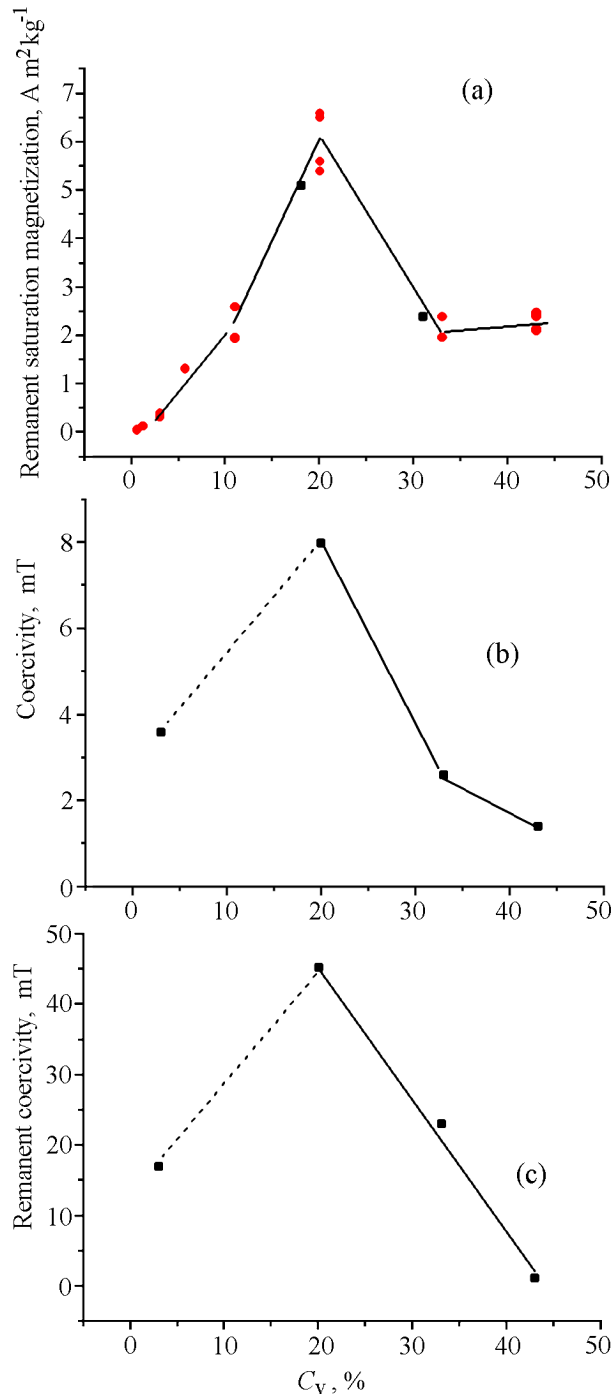


**Figure 7.** Variation of the hysteresis characteristics of the films as a function of the concentration of nanoparticles: (a) remanent saturation magnetization,  $J_{rs}$ ; (b) coercive force,  $H_c$ ; (c) remanent coercive force,  $H_{cr}$ .

which also showed peaks at  $C_v = 20\%$ . The  $H_c$  and  $H_{cr}$  values measured in this study for the film with  $C_v = 3\%$  were found to be 3.6 mT and 17 mT, respectively. The low coercivity values seem to have been associated with the significant content of superparamagnetic grains at the low

maghemite concentrations observed in the spectrum of the sample concerned (Figure 1). The maximum  $H_c$  and  $H_{cr}$  values were found to be 8 mT and 45.3 mT, respectively, which are feasible for the magnetite-maghemite system, as follows from the highly variable published experimental values and theoretical estimates [Dunlop, 1981; Gendler et al., 2005; Goss, 1988; Moscovitz et al., 1989; Sato et al., 1987; Sohn et al., 1998]. These variations are associated with the fact that at constant temperature, coercivity is controlled by a large number of factors, such as, grains size the patterns of their distribution, their morphology, and structural defects, the external tension, and the magnetic anisotropy and interaction among the particles. All of these structural characteristics are controlled, in turn, by the type of their formation. For instance, the values of the coercivity,  $H_c$ , of bulk maghemite reside in the range of 25–40 mT [Sohn et al., 1998]. The theoretical  $H_c$  values, available for isotropic, single-domain grains with the predominance of magneto-crystalline anisotropy were found to be 15 mT for maghemite and 19 mT for magnetite. However, in the vicinity of the single-domain/superparamagnetic boundary ( $ds$ ), the calculations show the  $H_c$  value to be 6.7 mT for the particles with a size of 40 nm and  $ds = 30$  nm [Dunlop, 1981]. In the case of maghemite grains of 37 nm in size and of the growing relative content of superparamagnetic particles, the coercivity calculated by Goss [1988] was found to be 4 mT. The experimental  $H_c$  values obtained for the magnetite and maghemite synthesized from the iron salt solution, without adding any PVA, varied from 0 mT to 15 mT for the cubic particles ranging from 7.5 nm to 17 nm in size [Coey et al., 1972; Sato et al., 1987], and from 23 mT to 36 mT for the needle-shape particles about 100 nm long [Morrish and Yu, 1955]. In the case of the fine-dispersed maghemite, obtained from lepidocrocite as a result of its long low-temperature annealing, the resulting  $H_c$  and  $H_{cr}$  values were found to be 3 mT and 6 mT, respectively [Gendler et al., 2005]. The nanoclusters of maghemite particles with the size of 5 nm, contained in block copolymers, and the particles with a size of 8.5 nm, contained in ion-exchange resins, showed a pure superparamagnetic behavior, with the  $H_c$  values equal to zero at room temperature [Sohn et al., 1998]. The magnetite grains of  $40 \times 40 \times 60$  nm in size, from magnetotactic bacteria MV-1, isolated from sulfide-rich sediments of an estuarine salt marsh, showed the  $H_c$  and  $H_{cr}$  values to be 28.5 mT and 48.5 mT, respectively, and the behavior typical of that observed for the assemblages of noninteracting single-domain grains. In turn, the magnetite grains produced by iron-reducing bacteria GS-15, showed the  $H_c$  and  $H_{cr}$  values equal to 0.8 mT and 30 mT, respectively, and the behavior consistent with the effects of magnetostatic interaction because of the particle agglomeration [Moskovitz et al., 1989]. This significant difference in the coercivity of the bacterial magnetite can be explained by a difference in the spectra of the grain sizes: narrow in the former, and broad in the latter case with a great contribution of SP grains. A similar situation seems to be observed in the study films in the case of the low concentrations of nanoparticles and the significant content of SP-size grains. The factors responsible for the growth of remanent magnetization and coercivity in the sample with  $C_v = 20\%$  remain to be found. The only

one real experimental fact is the appearance in this sample spectrum of the unresolved sextets conforming to iron ions with the valence of 2.5 and lower. This suggests the presence of  $\text{Fe}^{2+}$  ions in the octahedral sublattice of spinel, which is known to increase the constant of magnetocrystalline anisotropy and, hence, the coercivity. However, the concentration of  $\text{Fe}^{2+}$  ions grows with the further growing  $C_v$  values and the amount of the superparamagnetic particles declines, while the coercivity declining as well, similar to the remanent magnetization. It can be assumed that at high  $C_v$  values the mechanism responsible for the coercivity decline is the factor of the growing magnetostatic interaction between the ultradispersed particles in the films depth.

[27] The measurements of the remanent magnetization acquired in the magnetic field of two orthogonal directions (parallel and perpendicular to the film plane) were used to study the  $J_{rs}$  anisotropic properties. It was found that, irrespective of the magnetizing field direction, the  $J_{rs_{max}}$  vector does not only resides in the film plane, but also has a preferable orientation in it. For instance, the results of measuring the  $J_{rs}$  vector component ratios, normalized for the  $\mathbf{J}_{rs_z}$  vector for the sample with  $C_v = 43\%$   $\text{Fe}_3\text{O}_4$ , were found to be as follows:  $J_{rs_x} : J_{rs_y} : J_{rs_z} = 50 : 3.5 : 1$  and  $10.6 : 2.4 : 1$  for the external field parallel to and perpendicular to the surface of the film, respectively. Figures 8a and 8b shows the values of the coefficients of the planar ( $k_p$ ) and linear ( $k_l$ ) anisotropy for the films of different compositions

$$(k_p = \sqrt{(J_{rs_x})^2 + (J_{rs_y})^2} / J_{rs_z}, k_l = J_{rs_x} / J_{rs_y}).$$

One can see in Figure 8 that the planar anisotropy of all films compositions is higher than 10 and amounts to 50–55 for the  $C_v$  values higher or equal to 20% for the magnetization parallel to the plane surface. The  $k_p$  values declined by a factor of five for a sample with  $C_v = 43\%$ , in the case of the magnetization perpendicular to the film surface, yet remained to be significantly higher than 1 ( $k_p = 10.5$ ). The linear anisotropy was usually weaker than the planar one ( $k_l$ ): the  $k_l$  value varied averagely from 4 to 6 in the case of the magnetization parallel to the film surface for the  $C_v$  value lower than or equal to 33% and was found to be as high as 13.4 for a sample with the  $C_v$  concentration equal to 43% (see Figure 8b). Although the values of the linear anisotropy varied from 20% to 25% for different segments of the film and for different syntheses, yet, always remained to be higher than 1. Proceeding from the results of our measurements of  $J_{rs}$  anisotropy, we proposed the heterogeneous, lamellar-like or chain-shaped structure of the nanoparticles originating in the film depth parallel to the film surface. In other words, the anisotropy might have been caused by some magnetic texture produced by the active role of the organic nonmagnetic matrix in which nanoparticles are synthesized.

[28] Since the synthesis of the polymer nanocomposite material was carried out in the laboratory ambient magnetic field, it was of interest to check whether the magnetization acquired in the magnetic field of the Earth remained to be fixed in spite of the long procedure of the long washing with water during the synthesis. For this purpose we measured the natural remanent magnetization of the films [Gendler *et al.*, 2004]; this magnetization has been referred to above

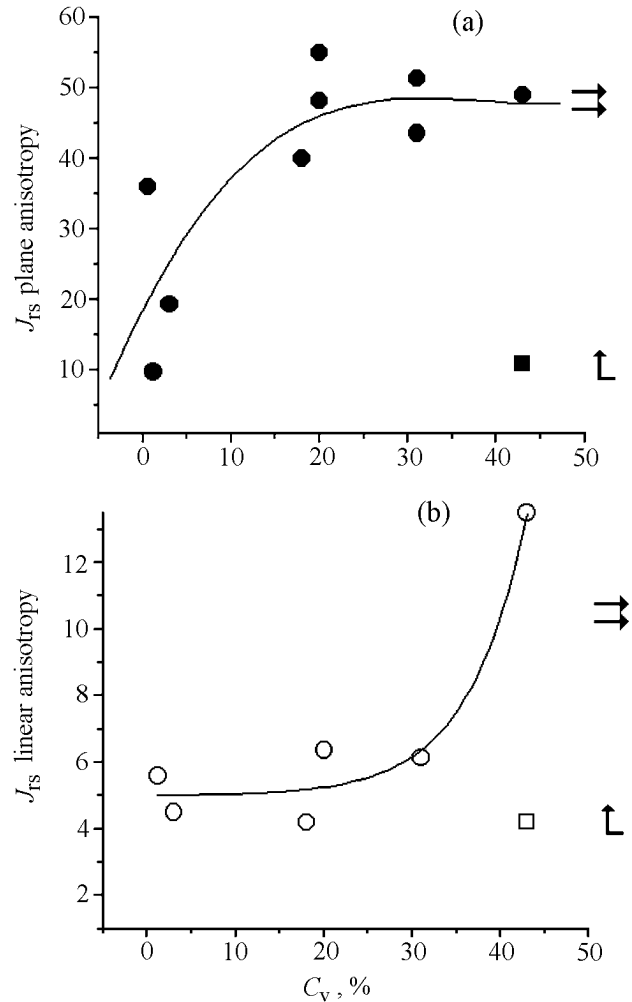


**Figure 8.** Anisotropy of the remanent saturation magnetization  $J_{rs}$  of the films with different concentrations of nanoparticles  $C_v$ : (a) planar  $J_{rs}$  anisotropy, (b) linear  $J_{rs}$  anisotropy. The solid and empty circles denote the external field parallel to the film surface, the solid and empty squares denote the external field perpendicular to the film surface.

as laboratory synthesis magnetization (LSM). As far as we know, those were the first LSM measurements in nanocomposite materials.

[29] In our case all samples were found to show LSM with its specific values varying from  $0.08 \cdot 10^{-2}$  to  $18 \cdot 10^{-2} \text{ Am}^2 \text{ kg}^{-1}$  calculated for the real content of magnetite. This means that the magnetic structure responsible for the interaction among the nanoparticles is forming as early as during the synthesis with the indisputable role of the polymer.

[30] The scatter of the LSM values measured for the samples of the same composition, but taken from different parts of the film, was found to be higher than the differences associated with changes in the film composition. Therefore we did not find any LSM variations produced by changes in the film composition, considering the limited amount of the

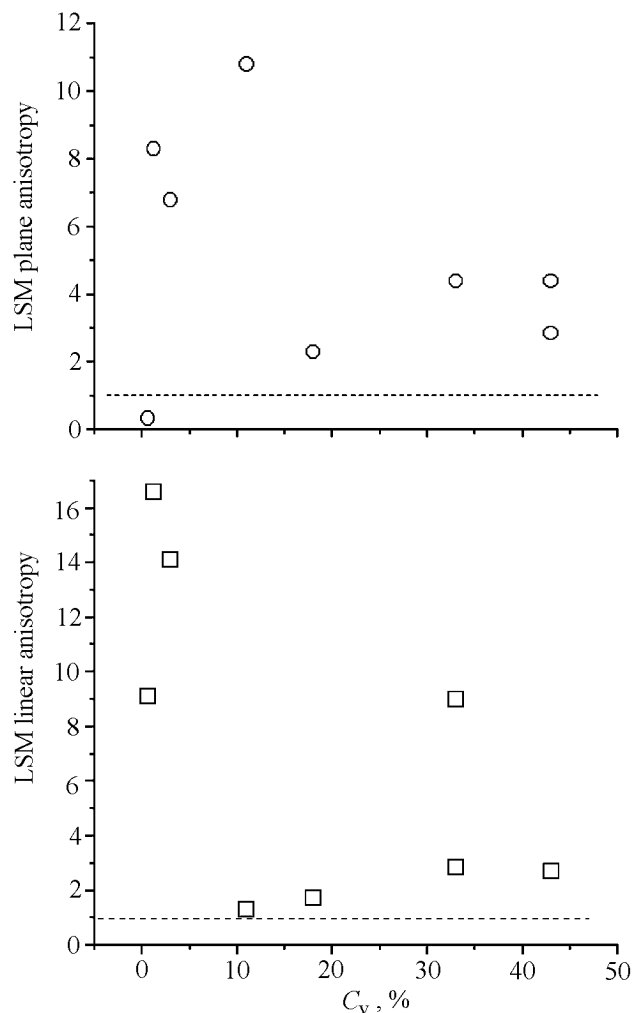


**Figure 9.** Anisotropy of laboratory synthesis magnetization (LSM). The empty circles are given for planar anisotropy, the empty squares, for linear anisotropy.

material obtained in each synthesis, available for our measurements.

[31] The laboratory synthesis magnetization (LSM) showed distinctly expressed anisotropy, similar to the remanent magnetization acquired in the magnetic field of 450 mT. The parameter of planar anisotropy  $k_p$  for the  $C_v$  concentrations ranging from 1.2% to 43% was substantially higher than 1, varying nonmonotonically over the range of 2 to 11 (Figure 9). Therefore the total vector of natural remanent magnetization acquired by polymer films in the course of the synthesis performed in the laboratory conditions in the Earth magnetic field resides primarily in the film plane for all concentrations beginning with  $C_v = 1.2$ . The exception was a sample with the lowest  $C_v$  concentration equal to 0.6%, which showed  $k_p = 0.34$ , that is, the LSM vector was perpendicular to the film plane. The aim of the next step was to calculate the coefficient of linear anisotropy,  $k_1$ . It was found that in the cases of all concentrations  $k_1$  was higher than 1 and varied from 1.1 to 16.6 depending on the film composi-

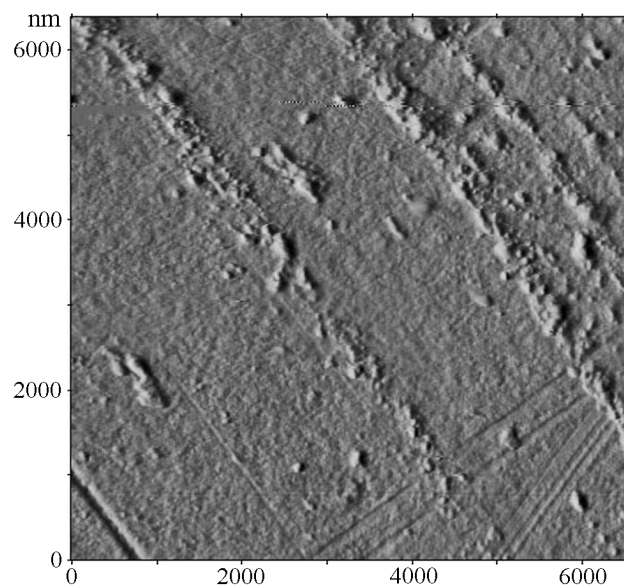


**Figure 10.** The AFM image of the lower surface of the film with  $C_v = 33\%$ , obtained using an atomic force microscope (AFM image), the size of the image being  $6 \times 6 \mu\text{m}$ .

tion (Figure 9). The highest values of the anisotropy were found for the lowest concentrations of nanoparticles, this having been potentially associated with large errors in measuring low LSM values, and calling for checking. Therefore the total vector of the remanent magnetization acquired by polymer films of all concentrations, beginning with  $C_v = 1.2$ , during the laboratory synthesis in the Earth magnetic field, lies not only in the film plane, but also along its certain axis. This suggests the formation of chain-type structures of nanoparticles in the Earth magnetic field at the expense of the PVA organizing role. It would be useful to verify the presence or absence of this structure using a similar synthesis in a screened off space and in the magnetic field of some fixed trend direction.

[32] The direct observation of the chain structures inferred from the magnetic measurements of chain structures was performed using a Femto Scan probing microscope, operating as an atomic-force microscope in the Center of Advanced Technologies, Moscow, [Novakova *et al.*, 2005a, 2005b]. Presented in Figure 10 is a photograph of the lower surface of the film ( $C_v = 33\%$ ), borrowed from these papers. In the case of large scales ( $\sim 6 \mu\text{m}$ ) one can see the rows of clustered particles arranged in one direction. Judging by their contrasting behavior, these rows are located at different depths below the sample surface. Moreover, they are scarce at the surface of the sample and grow in number with its depth, this being in agreement with the results of Mössbauer spectroscopy. The distances between the nearest parallel rows of the particles, lying in the same plane, vary within 200–400 nm, the thickness of the polymer envelopes between the nanoparticles ranging from 8 nm to 10 nm.

## Conclusion

[33] The results of this study show that during the synthesis of polymer films the nanoparticles of magnetite are distributed over the matrix in the heterogeneously manner. They remain almost noninteracting and supermagnetic in the vicinity of the surface of the film, yet in the film itself they produce layers with chain structures, parallel to the film plane, similar to those developed in magnetotactic bacteria. The stability of these chain structures is controlled by the dipole-dipole interaction among the nanoparticles, performed via the polymer matrix at the expense of the elastic energy of the envelopes of the organic matter separating the particles. The result of this mechanism is the possibility of the formation of a specific domain structure and the fixing of the natural remanent magnetization in the ensemble of the superparamagnetic nanoparticles. As follows from the paper by Jianbao *et al.* [2000], along with the growth of the pressure applied to the maghemite particles covered by surfactant envelopes, the blocking temperature increased significantly in association with the growing magnetic interaction among the particles. In a composite material, its matrix ensured not only the solidity of the material but was also responsible for stress distribution at the expense of the interaction between the matrix and the filling material at the phase contacts. As to the nanocomposite material discussed, where nanoparticles were synthesized *in situ* in a nonmagnetic polymer matrix, the polymer elastic forces produce stress at the particle surface, similar to the external pressure. This stress arising in the space between the particles, filled with polymer molecules, leads to the growth of microstress in the particles themselves, recorded by X-ray diffraction. The further convergence of the particles and the elastic energy of the matrix create conditions favorable for high magnetic interaction among the superparamagnetic particles, which fixes magnetization with blocking temperature of about 300°C.

[34] Shcherbakov *et al.* [1997] calculated the contribution of the elastic energy of envelopes from two-layer lipid membranes, 6 nm thick, to the stability of the chain structure of single-domain magnetite particles in magnetotactic bacteria. This problem can be transformed to a chain of superparamagnetic particles, separated by a PVA matrix, and this artificial system can be ranked as an analog of the biofilm produced by a colony of Fe-bacteria at the surface of minerals, where the bacteria become static. This result is important also for a new view for the formation of chemical remanent magnetization in nature, controlled by solutions. For instance, the laboratory experiments with amorphous ferric hydroxide, placed in the environment consisting of underground water, the samples of which had been collected from the overlying Cubero Sandstone, and the bacteria obtained from subsurface core samples (250 m below the ground surface) from the Morrison Formation, showed the substantial microbe recovery of the Fe(III) ions to their Fe(II) form [Fredrikson *et al.*, 1998]. The primary reduction products of amorphous iron hydroxide (30% to 84%), produced during the incubation of 3 to 25 days, were siderite grains, 1  $\mu\text{m}$  to 3  $\mu\text{m}$  in size, vivianite crystals, 5–10  $\mu\text{m}$

long and 0.5–1  $\mu\text{m}$  wide, and the aggregates of magnetite grains of a few nanometers. The substantial magnetic interaction among magnetite particles in the aggregates of this kind might have been caused or intensified by the organic material of the cells. As follows from the results of this study, this interaction might have contributed to the stable natural remanent magnetization in the ambient geomagnetic field without the growth of the particles necessary for the record of the magnetic field that existed during the time of their formation.

## References

- Araki, H. (1989), Micro-area X-ray diffraction techniques, *The Rigaku J.*, 6(2), 34.
- Berkowitz, A. E., W. J. Schuele, and P. J. Flanders (1968), Influence of crystallite size on the magnetic properties of acicular  $\gamma\text{Fe}_2\text{O}_3$  particles, *J. Appl. Phys.*, 39, 1261.
- Coey, J. M. D., and D. Khalafalla (1972), Superparamagnetic  $\gamma\text{Fe}_2\text{O}_3$ , *Phys. Status Solidi A.*, 11, 229.
- DeLong, E. F., R. B. Frankel, and D. A. Bazylinski (1993), Multiple evolutionary origins of magnetotaxis in bacteria, *Science*, 259, 803.
- Dunlop, D. J. (1981), The geomagnetism of fine particles, *Phys. Earth Planet. Inter.*, 26, 1.
- Evans, M. E., and F. Heller (2003), *Environmental Magnetism, Principles and Applications*, 295 pp., Acad. Press, USA.
- Fassbinder, J. W. E., H. Stanjek, and H. Vali (1990), Occurrence of magnetic bacteria in soils, *Nature*, 343, 161.
- Fredrickson, J. K., J. M. Zachara, D. W. Kennedy, H. Dong, T. C. Onstott, N. W. Hinman, and S. Li (1998), Biogenic iron mineralization accompanying the dissimilatory reduction of hydrous ferric oxide by a groundvarve bacterium, *Geochim. Cosmochim. Acta*, 62(19/20), 3239.
- Gendler, T. S., A. A. Novakova, and E. V. Smirnov (2004), Magnetic properties of polymer nanocomposites containing magnetite nanoparticles, in *Paleomagnetism and Rock Magnetism: Theory, Experiments, and Application*, p. 144, Kazan University Publ., Kazan.
- Gendler, T. S., V. P. Shcherbakov, M. J. Dekkers, A. Gapeev, S. K. Gribov, and E. McClelland (2005), The lepidocrocite-maghemite-hematite reaction chain: 1. Acquisition of chemical remanent magnetization by maghemite: Its magnetic properties and thermal stability, *Geophys. J. Int.*, 160, 815.
- Gibbs-Eggar, Z., B. Jude, J. Dominik, J. L. Loizeau, and F. Oldfield (1999), Possible evidence for dissimilatory bacterial magnetite dominating the magnetic properties of recent lake sediments, *Earth Planet. Sci. Lett.*, 168(1–2), 1.
- Goss, C. J. (1988), Saturation magnetization, coercivity, and lattice parameter change in the system of  $\text{Fe}_3\text{O}_4$ - $\gamma\text{Fe}_2\text{O}_3$ , and their relationships to structure, *Phys. Chem. Miner.*, 16, 164.
- Han, D. H., J. P. Wang, and H. L. Luo (1994), Crystalline size effect on saturation magnetization of fine ferrimagnetic particles, *J. Magn. Magn. Mater.*, 136, 176.
- Hancock, R. E. W. (2001), A brief on bacterial biofilms, *Nature Genetics*, 29, 360.
- Haneda, K., and A. H. Morrish (1977), Vacancy ordering in  $\gamma\text{Fe}_2\text{O}_3$  small particles, *Solid State Commun.*, 22, 779.
- Jakson, M., and S. Banerjee (2004), Santa Fe-VI, *The IRM Quarterly*, 14(1), 1.
- Jianbao, D., W. Jian-Qing, C. Sangregorio, F. Jiye, E. Crpente, and J. Tang (2000), Magnetic coupling induced the growth of magnetic coupling induced the growth of blocking temperatures in  $\gamma\text{Fe}_2\text{O}_3$  nanoparticles, *J. Appl. Phys.*, 87(10), 7397.
- Jolivet, J. P., P. Belleville, E. Tronc, and J. Livage (1992), Influence of Fe(II) on the formation of spinel iron oxide in alkaline medium, *Clays Clay Miner.*, 40(5), 531.

- Krumbein, W. E., D. M. Paterson, and G. A. Zavarzin (2003), Fossil and Recent Biofilms, *Biofilms*, Springer Academic Publ., Berlin.
- Kuprin, A. P., and A. A. Novakova (1992), Depth-selective  $^{57}\text{Fe}$  CEMS (DCEMS) on samples with rough surface using gas flow proportional counter, *Nucl. Instrum. Methods Phys. Res. B*, *62*, 493.
- Morrish, A. H., and S. P. Yu (1955), Dependence of the coercive force on the density of some iron oxide powders, *J. Appl. Phys.*, *26*, 1049.
- Mørup, S. (1990), Mössbauer effect in small particles, *Hyperfine Interact.*, *60*, 959.
- Moskowitz, B., R. Frankel, D. Bazylinski, and H. Jannasch (1989), A comparison of magnetic particles produced anaerobically by magnetotactic and dissimilatory iron-reducing bacteria, *Geophys. Res. Lett.*, *16*, 665.
- Novakova, A. A., T. S. Gendler, and N. A. Brusentsov (1992), The Mössbauer spectroscopic study of the properties of magnetic carriers for medicine, *Hyperfine Interact.*, *71*, 1315.
- Novakova, A. A., V. Yu. Lanchinskaya, A. V. Volkov, T. S. Gendler, T. Yu. Kiseleva, M. A. Moskvina, and S. B. Zevin (2002), Magnetic properties of polymer nanocomposites containing iron oxide nanoparticles, *Intern. Conf. on the Physics of Electronic Materials, Kaluga, 01-04 October, 2002*, p. 324, Abstract, Kaluga.
- Novakova, A. A., V. Yu. Lanchinskaya, A. V. Volkov, T. S. Gendler, T. Yu. Kiseleva, M. A. Moskvina, and S. B. Zevin (2003), Magnetic properties of polymer nanocomposites containing iron oxide nanoparticles, *J. Magn. Magn. Mater.*, *258-259*, 354.
- Novakova, A. A., T. S. Gendler, V. Yu. Lanchinskaya, E. V. Smirnov, A. V. Volkov, and M. A. Moskvina (2005a), Magnetic properties dependence on iron oxide nanoparticles concentration in polymer nanocomposites, *American Inst. of Physics AIP Conference Proceeding*, *765*, 273.
- Novakova, A. A., T. S. Gendler, E. V. Smirnov, A. V. Volkov, G. B. Meshkov, and I. V. Yaminskyi (2005b), Magnetic anisotropy forming at the synthesis of polymer nanocomposites, *Izv. Akad. Nauk, Ser. Fiz.* (in Russian), *69*(4), 675.
- Pankhurst, Q. A. (1994), The magnetism of the fine particles of iron oxides and oxihydroxides in applied fields, *Hyperfine Interact.*, *90*, 201.
- Peck, J. A., and J. W. King (1996), Magnetofossils in the sediments of Lake Baikal, Siberia, *Earth Planet. Sci. Lett.*, *140*, 159.
- Rudee, M. L., D. T. Margulies, and A. E. Berkowitz (1997), Antiphase domain boundaries in thin films of magnetite, *Microscopy and Microanalysis*, *3*(2), 126.
- Sato, T., T. Iijima, M. Seki, and N. Inagaki (1987), Magnetic properties of ultrafine ferrite particles, *J. Magn. Magn. Mater.*, *65*, 252.
- Shcherbakov, V. P., and M. Winklhofer (1997), Elastic stability of chains of magnetosomes in magnetotactic bacteria, *Eur. Biophys. J.*, *26*, 319.
- Sohn, B. H., R. E. Cohen, and G. C. Papaefthymiou (1998), Magnetic properties of iron oxide nanoclusters in microdomains of block polymers, *J. Magn. Magn. Mater.*, *182*, 216.
- Tarduno, J. A., W. Tian, and S. Wilkison (1998), Biogeochemical remanent magnetization in pelagic sediments of the western equatorial Pacific Ocean, *Geophys. Res. Lett.*, *25*(21), 3987.
- Voogt, F. C., T. T. M. Palstra, L. Niesen, O. C. Rogojuanu, M. A. James, and T. Himba (1998), Superparamagnetic behavior of structural domains in epitaxial ultrathin magnetite films, *Phys. Rev. B*, *57*(14), R8107.
- Zheng, M., X. C. Wu, B. S. Zou, and Y. J. Wang (1998), Magnetic properties of nanosized  $\text{MnFe}_2\text{O}_4$  particles, *J. Magn. Magn. Mater.*, *18*, 152.

---

T. S. Gendler, Institute of Physics of the Earth, Russian Academy of Science, 10 Bol'shaya Gruzinskaya ul., Moscow, 123995 Russia

A. A. Novakova, Lomonosov State University, Department of Physics, Vorobjovi Gori, Moscow, 119899 Russia

E. V. Smirnov, Semenov Institute of Chemical Physics, Russian Academy of Science, 4 Kosygin ul., Moscow, 117977 Russia